Topology Optimization: Applications of VFLSM and SESO in the Generation of Three-Dimensional Strut-and-Tie Models

By Hélio Luiz Simonetti, Valério S. Almeida, Virgil Del Duca Almeida, Luttgardes de Oliveira Neto, Marlan D. S. Cutrim & Vitor Manuel A. Leitão

University of São Paulo (EPUSP)

Abstract- This article presents the analysis of Strut-and-Tie Model (STM) in reinforced concrete 3D structures based on the study of topological optimization, so that the problem is formulated with the Smooth-ESO (SESO) discrete method, whose removal heuristic is bidirectional with discrete optimization procedure, and the Velocity Field Level Set Method (VFLSM), which is an inheritance of the classical continuum Level Set Method (LSM), but advances the design limits with a velocity field constructed from the rate of the design variables and base functions. The proposed approach is to couple both methods in conjunction with the Method of Moving Asymptotes (MMA), used to control the various design constraints that are the minimization of compliance and the Von Mises stress that has demonstrated more rational STM results. Additionally, it has been formulated a methodology for the automatic generation of optimal of 3D STM by using sensitivity analysis obtaining via derivatives of the Von Mises stress fields, finding the force paths prevailing compression in the directions of the strut and the tensile in the directions of the ties for the reinforcement insertion.

Keywords: reinforced concrete, topology optimization, strut-and-tie model, SESO, VFLSM.

GJRE-E Classification: DDC: 624

TOPOLOGYOPTIMIZATIONAPPLICATIONSOFVFLSMANDSESOINTHEGENERATIONOFTHREEDIMENSIONALSTRUTANDTIEMODELS

Strictly as per the compliance and regulations of:

Topology Optimization: Applications of VFLSM and SESO in the Generation of Three-Dimensional Strut-and-Tie Models

Hélio Luiz Simonetti [α], Valério S. Almeida [σ], Virgil Del Duca Almeida [ρ], Luttgardes de Oliveira Neto [ω], Marlan D. S. Cutrim [¥] & Vitor Manuel A. Leitão [§]

Abstract- This article presents the analysis of Strut-and-Tie Model (STM) in reinforced concrete 3D structures based on the study of topological optimization, so that the problem is formulated with the Smooth-ESO (SESO) discrete method, whose removal heuristic is bidirectional with discrete optimization procedure, and the Velocity Field Level Set Method (VFLSM), which is an inheritance of the classical continuum Level Set Method (LSM), but advances the design limits with a velocity field constructed from the rate of the design variables and base functions. The proposed approach is to couple both methods in conjunction with the Method of Moving Asymptotes (MMA), used to control the various design constraints that are the minimization of compliance and the Von Mises stress that has demonstrated more rational STM results. Additionally, it has been formulated a methodology for the automatic generation of optimal of 3D STM by using sensitivity analysis obtaining via derivatives of the Von Mises stress fields, finding the force paths prevailing compression in the directions of the strut and the tensile in the directions of the ties for the reinforcement insertion. All the codes are implemented with Matlab software and several comparison examples: Deep beam with opening, a pile cap, a bridge pier, and a single corbel, are presented to validate the present formulations and the results are compared with the literature.

Keywords: reinforced concrete, topology optimization, strut-and-tie model, SESO, VFLSM.

I. Introduction

In the field of structural engineering, most concrete linear elements are designed by the classical theory of Bernoulli hypothesis. For a real physical analysis about behavior of these bending elements it is common to use the Strut-and-Tie Model (STM) that is a generalization of the classical analogy of the truss beam model. This analogy is shown by Ritter and Morsch at the beginning of the twentieth century, associated with the Reinforced Concrete (RC) beam in an equivalent truss structure (regions B, Fig. 1). The bar elements represent the fields of tensile and the compressed struts emerged inside the structural element as bending effects. The analogy has been improved and is still used by the technical standards in the design of reinforced concrete beams in flexural and shear force and laying down various criteria for determining safe limits in its procedures. However, the application of this hypothesis for any structural element can lead to over or under sizing of certain parts of the structure.

The Bernoulli hypothesis is valid for parts of the frame that there is no interference from other regions, such as sections near the columns, changing in geometry or other areas where the influence of strain due to shear efforts is not negligible. In this line, there are regions where the assumptions of Bernoulli do not adequately represent the bending structural behavior and the stress distribution. Structural elements such as beams, walls and pile caps and special areas such as beam-column connection, openings in beams and geometric discontinuities are examples. These regions, denominated "discontinuity regions D", are limited to distances of the dimension order of structural adjacent elements (Saint Venant's principle), that the shear stresses are applicable and the distribution of strains in the cross section is not linear. From the 80's, a Professor at the University of Stuttgart and other collaborators presented several researches that evaluated these regions more adequately, as [1], [2], [3], and other researchers as [4], [5] and [6]. The pioneering work by [1] describes the STM more generally, covering the equivalent truss models and including these regions and special structural elements. The analogy used in the STM uses the same idea of the classical theory in order to define bars representing the flow of stress trying to create the shortest and more logical path loads. Several experimental evaluations have been studied to validate the STM applied to the RC design, as [7], [8], [9] and [10].

Author α: Ph.D, Department of Mathematics, Instituto Federal de Educação, Ciência e Tecnologia de Minas Gerais IFMG.
e-mail: helio.simonetti@ifmg.edu.br

Author σ: Ph.D, Department of Geotechnical and Structural Engineering, School of Engineering, University of São Paulo (EPUSP).
e-mail: valerio.almeida@usp.br

Author ρ: MSc, Department of Automation and Control Engineering, Instituto Federal de Educação, Ciência e Tecnologia de Minas Gerais – IFMG. e-mail: virgil.almeida@ifmg.edu.br

Author ω: Doctor, Department of Civil and Environmental Engineering - School of Engineering –UNESP. e-mail: lutt@feb.unesp.br

Author ¥: MSc, Department of Structure Engineering and Geotechnics of the Polytechnic School of the University São Paulo –USP.
e-mail: marlancutrin@usp.br

Author §: Prof. Doctor, CERIS, Instituto Superior Técnico, Universidade de Lisboa. e-mail: vitor.leitao@tecnico.ulisboa.pt

The STM is recognized as a rational approach to the design of discontinuity regions and is incorporated in several current codes, such as ASCE-ACI 445 on Shear and Torsion [11], [12], [13] and [14]. These code provisions still require improvement due to uncertainties in the selection of optimal struts-and-ties, especially in the case of complex geometry or general load application conditions. Because of its simple model and needs the experience of the designer to select and distribute the elements of the model in order to represent the stresses path in a better way, it becomes evident the use of more reliable and automatic tools for defining its geometric and structural configuration.
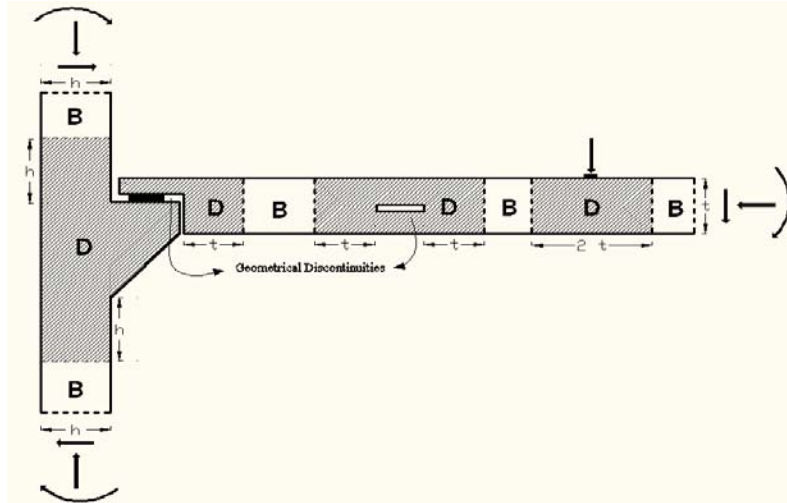

Fig. 1: D and B regions

To overcome these difficulties and improve the efficiency in building the optimal STM in RC structures, the theory of Topology Optimization (TO) has been used for two decades as an alternative and systematic approach consolidating itself as a fruitful path of design related research, once facilitates the shaping of materials under certain conditions. Many methods have been proposed for the solution of TO applied to STM, highlighting the use of the classical SIMP: [15], [16], [17], or ESO (Evolutionary Structural Optimization): [18], [19], [20], Liang et al. [21,22,23], Chen et al. [24], Zhong et al. [25], or variants, like BESO, Shobeiri et al. [26], RESO (Refined ESO), Leu et al. [27] or SESO proposed by the present authors, Almeida *et al.* [28]. SESO is based on the philosophy that if an element is not really necessary for the structure, its contribution to the structural stiffness is gradually diminished until it does not have any influence in the structure; that is, its removal is done smoothly, not radically as in the ESO method, that have been showed more efficient and robust and less sensitive to the discretization than ESO and faster than BESO, causing a decrease of the checkerboard formation.

In the last decade, the Level Set Method (LSM) has been highlighted in the field of TO, different from the conventional element wise density-based methods. LSM has clearer and smoother results and are flexible for complex topological changing, citing the pioneer's works of [29], [30] and [31]. The method describes the topological path by an implicit shape evolutive sequence by using a higher dimensional function to the design space for achieving the minimum energy under design constraints. Several other schemes have been included in the standard LSM to improve performance and achieve better results for general applications, like [32], [33]. Wang and Kang [34,35] proposed the Velocity Field Level Set Method (VFLSM) which has been proved to be more efficient to deal with multiple constraints and design variables than LSM, but few works have been applied to STM by using VFLSM.

OT in solving problems in the field of 3D STM is not much explored for general D-regions, discouraged by the instabilities (checkerboard problem) inherent to SIMP, ESO/BESO or the complex formulation and high processing time of LSM/VFLSM. Thus, for stabilizing and accelerating the TO solution, several mathematical optimization methods have been proposed, such as Optimality Criteria, by Huang et al. [36] with BESO, Augmented Lagrangian [37] or [38] with Level-Set, Lagrangian multiplier by [39] and [40] with LSM, or the Method of Moving Asymptotes (MMA), by [41] with SIMP.

In the present work, aiming at the solution of 3D STM in general reinforced concrete problems, the SESO methods whose advantages are easy implementation and decrease of the checkerboard effect and the VFLSM, which deals well with shape and topological optimizations, are formulated together with the MMA optimization method to accelerate and stabilize 3D STM. It is also noteworthy new approach of sensitivity analysis is incorporated in these formulations for the automatic generation of struts-and-ties based on partial derivatives

with respect to Von Mises stresses. The volume constraints are considered in the analyses, as the implementation of a spatial filter and the conjugate gradient method with the incomplete Cholesky preconditioner to speed up the solution of the linear system of each step of the search.

a) *Problem Formulation*

Considering the classical topology problem for the maximum stiffness of statically loaded linear elastic structures, a TO mathematical formulation for continuum structure can be discussed. Considering the TO problem as minimizing the deformation energy of a given structure considering the equilibrium, it follows that W=2U. The problem can then be defined as:

$$\text{Minimize:} \quad U(X) = \frac{1}{2}u^T K u = \sum_1^{NE} \frac{1}{2} \int_{V_e} \varepsilon_e^T E_e(x)\varepsilon_e \, dV_e$$

$$\text{Subject to:} \quad Ku = F$$

$$V(X) = \sum_{i=1}^{NE} X_i V_i - \underline{V} \leq 0 \tag{1}$$

$$X = \{x_1 x_2 \ x_3 \ \dots \ x_n\}, \ x_i = 1 \ or \ x_i = 0$$

with E_e being the element's elasticity matrix, ε_e is the element's strain vector, V_e is the volume of an element, NE is the number of finite elements of the mesh, K is the stiffness matrix, $Ku = F$ is the equilibrium equation, F is the vector of loads applied to the structure, x_i is the design variable of the *i-th* element, X is the vector of design variables.

b) *Smooth Evolutionary Structural Optimization (SESO)*

The ESO method, which heuristic is based on the gradual and systematic removal of elements whose contribution to the stiffness of the structure are insignificant, was proposed by Xie and Steven [42]. The SESO method proposed by Simonetti et al. [43] is based on the ESO philosophy and applies a weighting to the constitutive matrix so that the element that would

be eliminated is maintained and receives a smoothing characteristic. This treatment procedure applies a degradation in the value of its initial stiffness in such, during the removal process, its influence can contribute and determine its permanence or its definitive withdrawal from the design domain. Thus, the elements located near the limit to the left of this maximum strain energy are kept in the structure, defining a smoother heuristic removal. In Fig. 2, $D(j)$ is the constitutive matrix of element j, $\Gamma = \Gamma_{LS} + \Gamma_{GS}$ is the domain of elements that can be withdrawn, Γ_{LS} is the domain of elements that must be effectively removed, Γ_{GS} is the domain of elements that are returned to the structure, $0 \leq \eta(\Gamma) \leq 1$ is a weighted function.
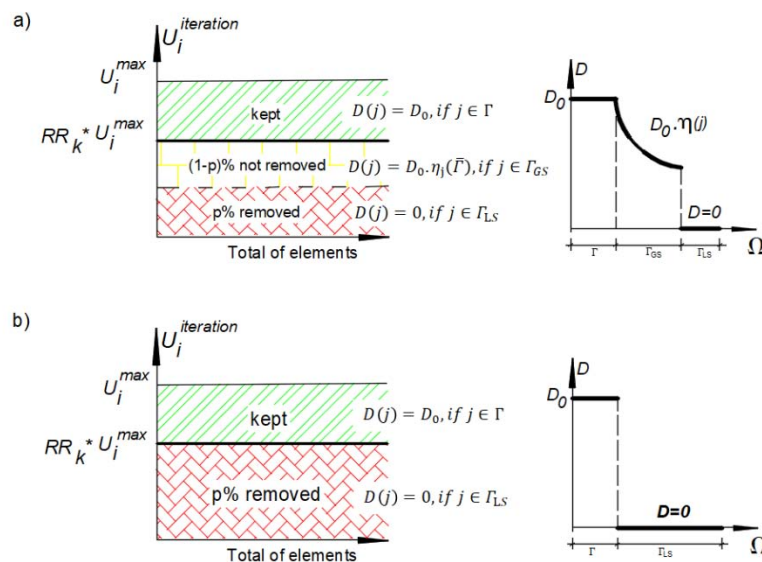

Fig. 2: Classic procedure in strain energy: (a) SESO and (b) ESO

c) *The Level Set Method (LSM)*

LSM is a technique for representing moving interfaces or boundaries using a fixed mesh. The dynamics of the interfaces can be formulated as the evolution of the level function defined by $\phi(x(t), t)$, which is continuous Lipschitz and is usually defined as follows

$$\phi(x,t) = \{ \phi(x,t) > 0 \ \ \forall \, x \in \Omega\backslash\partial\Omega \, ; \quad \phi(x,t) = 0 \ \ \forall \, x \in \partial\Omega \, ; \quad \phi(x,t) < 0 \ \forall \, x \in D\backslash\Omega \ \} \qquad (2)$$

with $x\epsilon D \subset \{(x,y)\epsilon R^2\}$ is any point in the design domain D and $\partial\Omega$ is the solid domain boundary as shown in Fig. 3 for a 2D case.

In classical LSM for TO, such as [30] and [31], the design evolution is based on the solution of the Hamilton-Jacobi partial differential Eq. (4). Thus, it needs an appropriate choice of finite difference methods on a fixed cartesian mesh. In general, the design update involves differentiation, resetting and velocity extension.

$$\frac{\partial\emptyset}{\partial t} - V_n|\nabla\emptyset| = 0 \qquad (3)$$

$$V_n = V.\left(-\frac{\nabla\emptyset}{|\nabla\emptyset|}\right) \qquad (4)$$

with $\nabla\emptyset$ denotes the gradient of a function, t is the pseudo time that represents the evolution of the function $\phi(x,t)$ defined, $V_n(x,t)$ is the normal velocity vector (pointing outwards) based on the derivatives of the shape functions in the TO problem.
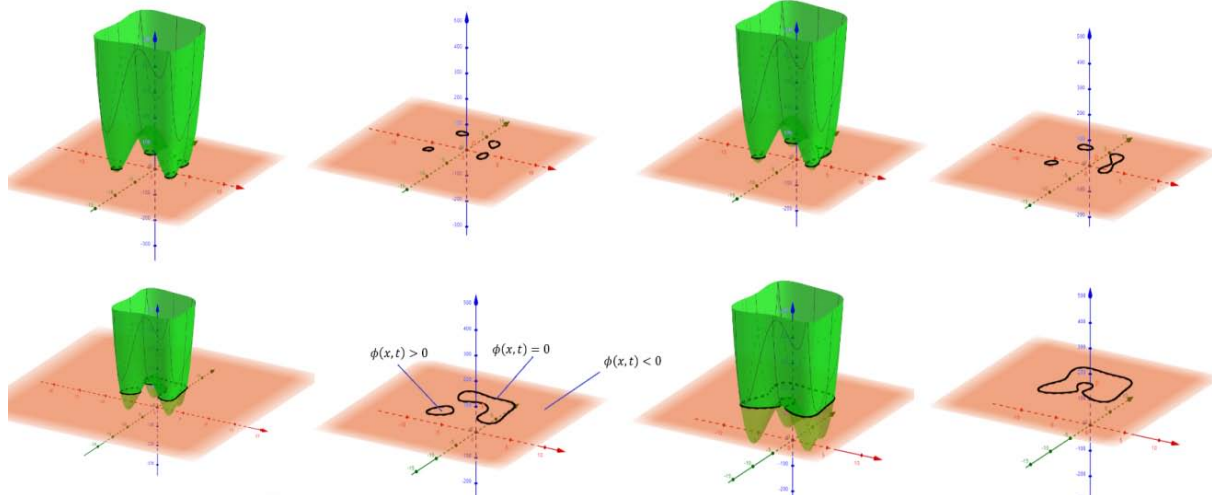

$\phi(x,t) > 0$ $\phi(x,t) = 0$ $\phi(x,t) < 0$

Fig. 3: Evolution history of the 2D geometry to a 3D level

Recently, Wang and Kang [34, 35] proposed a 100-line Velocity Field Level Set (VFLS), implemented in Matlab code. The structural shape and topology are updated by a velocity field constructed with the base function and velocity design variables defined throughout the domain. Then, the velocity field determines the search direction of the shape and the topological evolution can be obtained by a generic mathematical programming algorithm, which makes it more convenient and efficient to deal with multiple constraints and types of design variables. For VFLS, we have:

$$V_n(x) = \sum_{j=1}^{N} \beta_j \, p_j(x) \qquad (5)$$

with $\beta_j \, (j = 1,2,...,N)$ are the velocity design variables at N velocity points distributed throughout the main design, and $p_j(x)$ are the basic functions. It is observed that when p_j satisfies the properties of the Kronecker delta it has $\beta_j = V_n$ of Eq. (3).

II. Optimization Algorithm - Moving Asymptotes Method

To accelerate and stabilize the present 3D STM in this paper, MMA is employed, which is a mathematical programming algorithm suitable for TO, capable of handling optimization of many constraints and design variables. At each step of the algorithm's iterative process, a convex approximation subproblem is generated and solved. The generation of these subproblems is controlled by the moving asymptotes, which can both stabilize and accelerate the convergence of the overall process, [44].

The optimal solution of the subproblem may or may not be accepted: if so, the outer iteration is completed; if not, a new inner iteration is performed, in which a new subproblem is generated and solved. The iterations are repeated until the values of the approximations of the objective function and the constraints become greater than or equal to the values of the original function when evaluated in the optimal solution of the subproblem, that is, until the conservative condition is satisfied for the functions involved. The approximations that characterize the MMA are rational functions whose asymptotes are updated at each iteration. It is noteworthy that the use of rational approximations is justified by the fact that in several structural engineering problems where reciprocal variables arise, that is, interaction and mutual effort, given the objective function or a constraint $C(x)$, the approximation functions are given by:

$$C(x) \approx C(x^k) + \sum_1^n \left(\frac{r_i}{U_i^{(k)} - x_i} + \frac{s_i}{x_i - L_i^{(k)}} \right) \quad (6)$$

where r_i e s_i are defined as:

$$If \ \frac{\partial C(x)}{\partial x_i} > 0 \ then \ r_i = \left(U_i^{(k)} - x_i^{(k)}\right)^2 \frac{\partial C(x)}{\partial x_i} \quad and \quad s_i = 0 \quad (7)$$

$$If \ \frac{\partial C(x)}{\partial x_i} < 0 \ then \ s_i = -\left(x_i^{(k)} - L_i^{(k)}\right)^2 \frac{\partial C(x)}{\partial x_i} \quad and \quad r_i = 0 \quad (8)$$

For the optimization problem in compliance Eq. (8), it is known that it is satisfied because $\frac{\partial C(x)}{\partial x_i} < 0$. Then the MMA provides the current design with an approximation of a linear programming problem of the type:

$$Minimize \quad - \sum_1^n \frac{\left(x_i^{(k)} - L_i^{(k)}\right)^2}{x_i - L_i^{(k)}} \frac{\partial c}{\partial x_i}\left(\tilde{x}^{(k)}\right)$$

$$Subject \ to \quad \tilde{x}^T v - \underline{v} \leq 0 \quad (9)$$

$$x \in \chi^k$$

with $\chi^k = \{x\epsilon\chi | 0.9 L_i^{(k)} + 0.1 x_i^{(k)} \leq x_i \leq 0.9 U_i^{(k)} + 0.1 x_i^{(k)}\} \ \forall \ i = 1,2,\dots,n$

with $L_i^{(k)}$ and $U_i^{(k)}$ being lower and upper asymptotes, respectively, k is the current iteration, n the number of design variables, x^k the design variable and $\underline{v}$ the prescribed volume. The following heuristic rule is used by [44] for updating the asymptotes, for the first two outer iterations, when k =1 and k = 2 are adopted:

$$U_i^{(k)} + L_i^{(k)} = 2x_i^{(k)} \quad (10)$$

$$U_i^{(k)} - L_i^{(k)} = 1$$

For $k \geq 3$

$$U_i^{(k)} + L_i^{(k)} = 2x_i^{(k)}$$

$$U_i^{(k)} - L_i^{(k)} = \gamma_i^{(k)}$$

with

$$\gamma_i^{(k)} = \begin{cases} \zeta\left(x_i^{(k)} - x_i^{(k-1)}\right)\left(x_i^{(k-1)} - x_i^{(k-2)}\right) < 0 \\ \xi\left(x_i^{(k)} - x_i^{(k-1)}\right)\left(x_i^{(k-1)} - x_i^{(k-2)}\right) > 0 \\ \varsigma\left(x_i^{(k)} - x_i^{(k-1)}\right)\left(x_i^{(k-1)} - x_i^{(k-2)}\right) = 0 \end{cases} \quad (11)$$

where the values of ζ, ξ and ς were fitted in the respective numerical ranges $0.65 \leq \zeta \leq 0.75$, $1.15 \leq \xi \leq 1.25$ and $0.9 \leq \varsigma \leq 1$.

It can be seen in Eq. (11) that the MMA saves the signal of three consecutive iterations. Thus, when the signals alternate, the MMA detects that the values of the design variables are oscillating, i.e., $\left(x_i^{(k)} - x_i^{(k-1)}\right)\left(x_i^{(k-1)} - x_i^{(k-2)}\right) < 0$, the asymptotes

approximate the design point $x_i^{(k)}$. If the values of the design variables do not oscillate, i.e., $\left(x_i^{(k)} - x_i^{(k-1)}\right)\left(x_i^{(k-1)} - x_i^{(k-2)}\right) \geq 0$, then the MMA moves the asymptotes away from the design point in order to accelerate up convergence. There are two approaches to solving subproblems in MMA, the "dual approach" and the "primal-dual interior point approach". The dual approach is based on the dual Lagrangian relaxation corresponding to the subproblem, which seeks the maximization of a concave objective function without other constraints and the non-negativity condition on the variables. This dual problem can be solved by a modified Newton method, and then the dual optimal solution can be translated into a corresponding optimal solution of the primal subproblem, which is used in this paper.

III. METHODOLOGY FOR GENERATION 3D STRUT-AND-TIE MODELS AND THE FINAL FLOWCHART

To determine the path load of the 3D bars of the STM from the TO analysis, this paper employs a new procedure to evaluate the struts and ties by the signs of the derivatives of the Von Mises stress components. It is known that for 3D problems they can be written as

$$(\sigma_e^{vm})^2 = \frac{1}{2}[(\sigma_{11} - \sigma_{22})^2 + (\sigma_{22} - \sigma_{33})^2 + (\sigma_{33} - \sigma_{11})^2] + 3(\sigma_{12}^2 + \sigma_{23}^2 + \sigma_{31}^2) \quad (12)$$

Taking the local calculation of the derivative of the von Mises stress of the element with respect to the components of the stress vector described respectively as:

$$\frac{\partial(\sigma_e^{vm})}{\partial\sigma_{e11}} = \frac{1}{2\sigma_e^{vm}}(2\sigma_{e11} - \sigma_{e22} - \sigma_{e33})$$

$$\frac{\partial(\sigma_e^{vm})}{\partial\sigma_{e22}} = \frac{1}{2\sigma_e^{vm}}(2\sigma_{e22} - \sigma_{e11} - \sigma_{e33})$$

$$\frac{\partial(\sigma_e^{vm})}{\partial\sigma_{e33}} = \frac{1}{2\sigma_e^{vm}}(2\sigma_{e33} - \sigma_{e11} - \sigma_{e22}) \tag{13}$$

$$\frac{\partial(\sigma_e^{vm})}{\partial\sigma_{e12}} = \frac{3\sigma_{e12}}{2\sigma_e^{vm}}$$

$$\frac{\partial(\sigma_e^{vm})}{\partial\sigma_{e23}} = \frac{3\sigma_{e23}}{2\sigma_e^{vm}}$$

$$\frac{\partial(\sigma_e^{vm})}{\partial\sigma_{e31}} = \frac{3\sigma_{e31}}{2\sigma_e^{vm}}$$

Considering Eq.(13) and making $\frac{\partial(\sigma_e^{vm}(x))}{\partial\sigma_{e11}} > 0$ then the elements are preponderantly tensioned (blue color - ties) while $\frac{\partial(\sigma_e^{vm}(x))}{\partial\sigma_{e33}} < 0$ are preponderantly compressed (green color - strut). The flowchart presented in Fig. 4 shows the original methodology presented in this section with the approach of using element sensitivity for automatic generation of STMs via stress derivatives, when a target volume is reached, the stopping criterion is reached. A set of techniques has not yet been presented in scientific articles on 3D models, so the results obtained in item 4 are compared with those proposed by [16], [26] and [45]. Highlights that the VFLSM method required a neighborhood filter to define the tensile (blue) and compression (green) regions. This filter is due to intermediate values that occur in continuous TO methods such as the intermediate densities that occur in the SIMP methodology.

IV. Numerical Examples

The following examples of structures engineering focus on TO base on minimizing compliance for STMs. The geometry and boundary conditions for numerical applications are represented for each case. All numerical examples were processed on a Core i7-2370, 8th Gen notebook, 2.8 GHz CPU with 20.0 GB (RAM).

a) Example 1 – Deep Beam with Opening

The example presents a simply supported deep beam with an opening at the bottom left corner. The beam has its span three times its height and it is defined in [46], where the simple bending structural behavior is no longer considered. A vertical downward force F=3000 kN is applied eccentrically at the top edge as shown in Fig. 5. The structure is discretized with a total of 65,420 hexahedral elements (SESO) and 65,420 tetrahedral elements (LSM) (Fig. 5 shows the design domain and its boundary conditions). In this configuration, the force in off-center position and the opening positioned near the left low end create a situation that changes the internal stress flow in the structure, between the load and the supports. The tie elements, resulting from tensile stresses, are positioned at the extremities of the strut elements, resulting from compressive stresses, geometrically defining the final model.
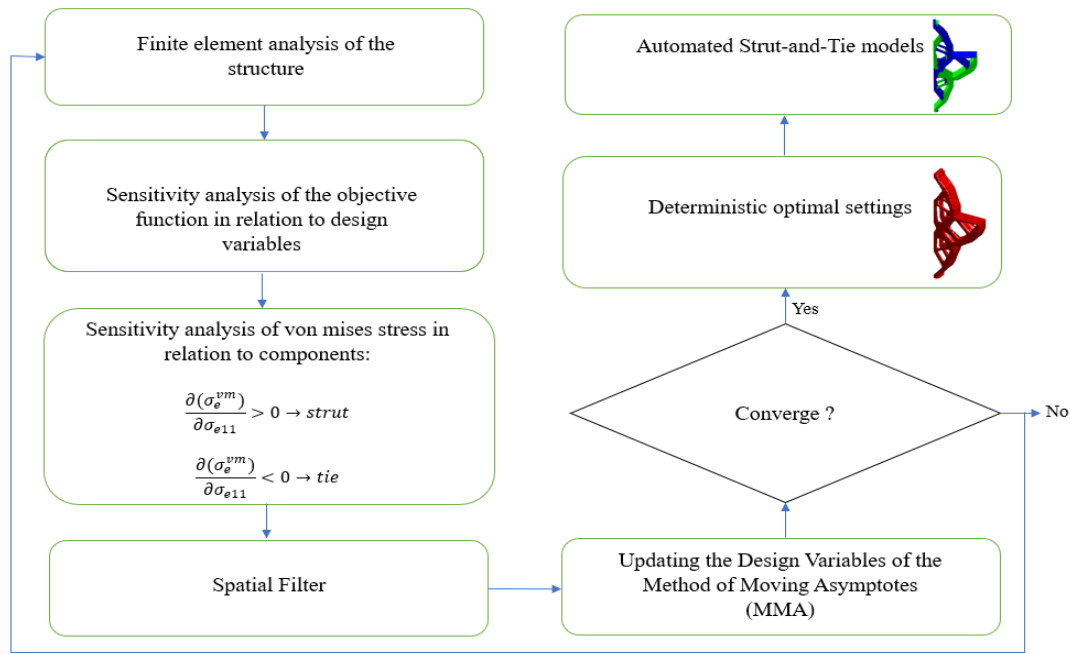
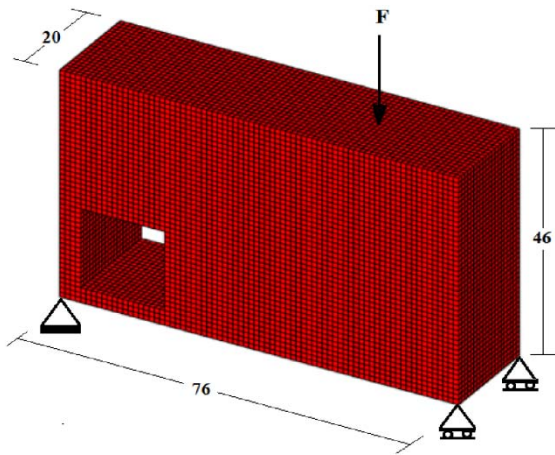Fig. 4: Flowchart of the STM via TO

Fig. 5: Design domain and boundary conditions (measuring in cm)

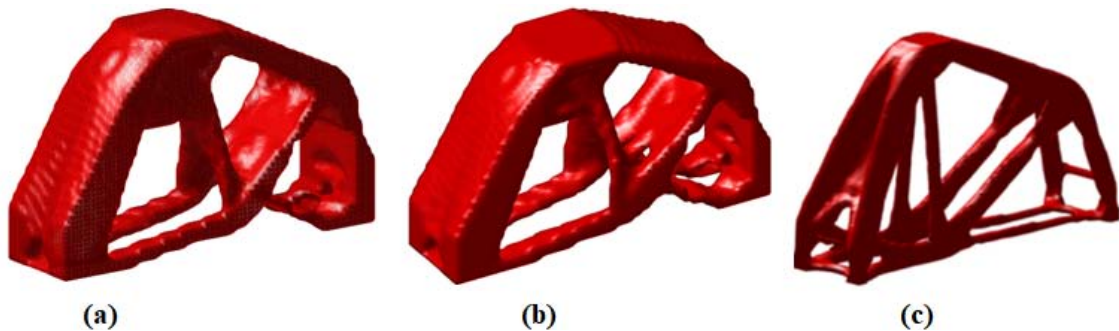Fig. 6 provides the optimal topologies of the optimization procedures for the SESO (Fig. 6a and Fig.

6b) and VFSLM (Fig. 6c) methods, with a final volume fraction equal to 32%. The optimal configurations have similarity to the classical STM presented by [1] and later by [20]. The computational cost presented by SESO using Optimality Criteria [47] is approximately 40% lower than the SESO and VFLSM methods using the MMA. It can be also noticed in Fig. 6 that the optimal settings obtained by the VFLSM formulation clearly defines distinct elements (strut or tie) near the lateral faces of the deep beam, resulting in a more discrete STM, compared to the optimal settings presented by the SESO method. The classic model, Fig. 7, denotes three diagonal struts starting from the region of load application, one of them external directed to the closest support, another contouring the opening and directed to the support, and a third internal one. The ends of the struts are connected by tie composing the final structure of the STM.
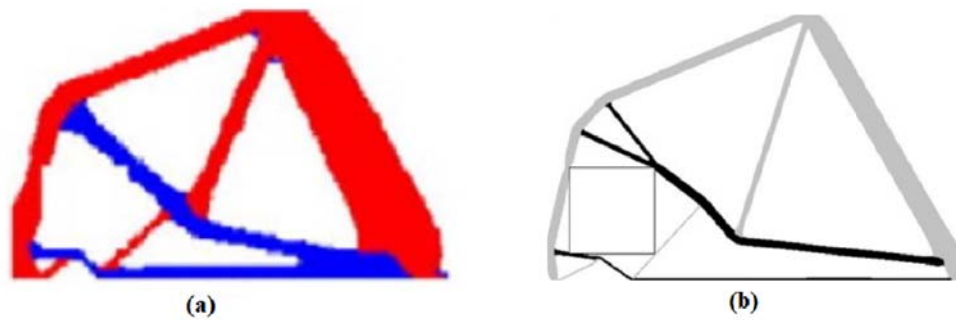

Fig. 6: Topology optimal for deep beam: (a) SESO-MMA; (b) SESO – OC and (c) VLSM-MMA

Fig. 7: Topology optimal for deep beam with opening: classical model (a) [28]; (b) [45]

In Fig. 8 it can be seen that the SESO formulation (Fig. 8a) results in a setting similar to the classical model, but the VFLSM formulation (Fig. 8b) presents a model with a discretely simpler setting, with the internal strut in the vertical direction, unifying at a lower point the two ties. This setting simplifies the design procedure and the reinforcement detailing of the reinforced concrete structure, in the practical and executive sense, although the classic model makes it possible to calculate the complementary reinforcement around the opening.
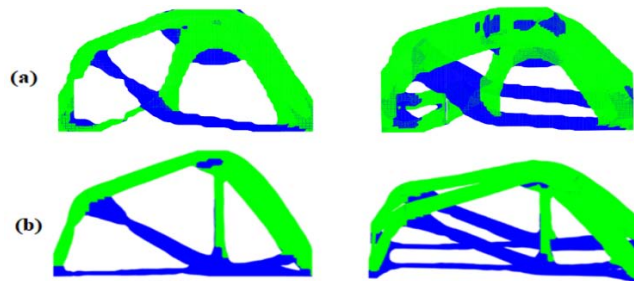
Fig. 8: Strut-and-tie models: (a) SESO; (b) VFLSM

b) Example 2 – Pile Cap

In this example, a building foundation structure is dimensioned as a pile cap according to the dimensions shown in Fig. 9, for consideration as a rigid block and to enable the analysis by the STM concept. The pile cap is subjected to a vertical force of 4,000 kN located at the center of the upper face. The material properties used are the compressive strength of the concrete cylinder is 32 MPa. The Young's modulus of the concrete E_c = 25,000 MPa and Poisson's coefficient $\nu = 0.15$. The filter radius $r_{min} = 1.5\ mm$ mm and the volume fraction of 22.5%, a rejection ratio, RR = 1% and the evolution ratio ER = 2% were specified in the optimization process.
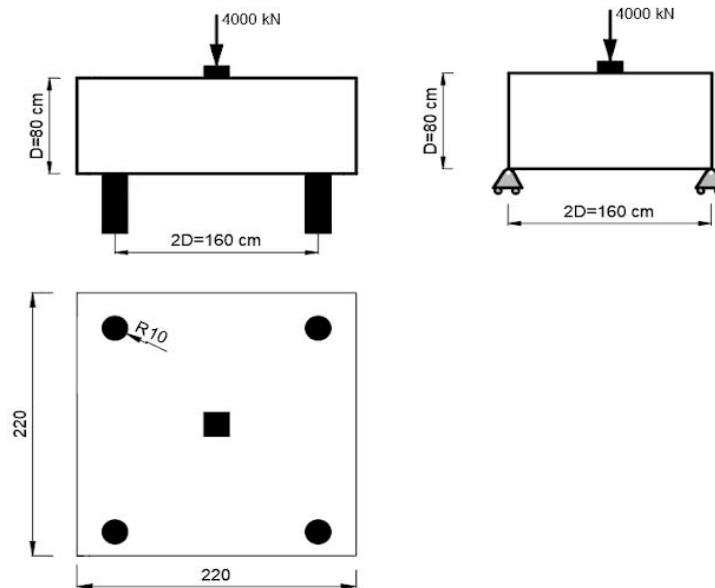
Fig. 9: Design domain and boundary conditions of pile cap

In the numerical simulations, to discretize the domain of the structure, a refined mesh of 40x20x40 was used, totaling 32,000 hexahedral elements (SESO) with 1mm reference side was used and a mesh of 32,000 tetrahedral elements (VFLSM). The results obtained as final optimal topologies of this problem for these meshes are represented in Fig. 10 and can be compared with the results with those presented by [16] and [26], see Fig. 11.

The optimal topology is basically composed of discrete elements represented in the principal stress flows. These optimal settings are adequate to perform the detailing and dimensioning of the required reinforcement, as well as strength checks. In this structure, the vertical load is distributed in four struts inclined toward the supports represented by vertical piles. The models highlight elements at the base of the pile cap, representing the tensile stresses, where a plane frame of ties balances the strut ends generated by the 3D structure in both horizontal directions, Fig. 10, where it can be seen the optimum topologies for the two methods, SESO and VFLSM. In the automatic generation of the strut models, it was considered the main flows of distinct stresses by colors, where the region of compression struts is green color and the region of tensile ties is blue.

a)   b)

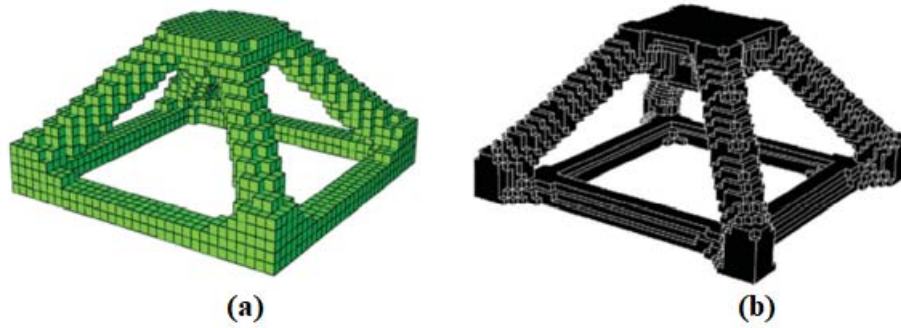Fig. 10: Optimal topology: (a) SESO; (b) VLSM (present formulation)

Fig. 11: Optimal topology: (a) BESO by [26]; (b) SIMP by [16]

Although the models result quite similar, when approaching this problem, one must consider the increased computational burden associated with a 3D structure; a solid mesh usually requires that many elements be investigated at an adequate level of detail, with notable consequences on the number of equations and variables. Seeking to minimize this aspect of the processing, the system of equations received the implementation of a sparse approximation preconditioner for the inverse matrix. With this routine active, the computational cost of SESO-3D for this problem was decreased from 8,000 sec to 1,854 sec (4.3 times less) while VFLSM had a decrease from 8,000 sec to 3,851sec (2.1 times less).

The dimensioning of the reinforcement of this model is performed, as already presented in [28]; in the calculations of the dimensions of the model elements, namely, inclined compression strut - column-pile and horizontal tension tie - pile-pile, the geometry of the problem presented [26] is used:

$$force\ in\ Strut - C_1 = \frac{\frac{4,000}{4}}{sin(29.5)} = 2,031\ kN$$

$$force\ in\ Tie - T_1 = C_1 \frac{cos(29.5)}{\sqrt{2}} = 1,250\ kN$$

Two evaluations need to be performed, the limits of stresses in the steel bars (CA50) for the tie and stresses in the concrete (C32) of the struts. According to the Brazilian technical standard, we have the following expressions:
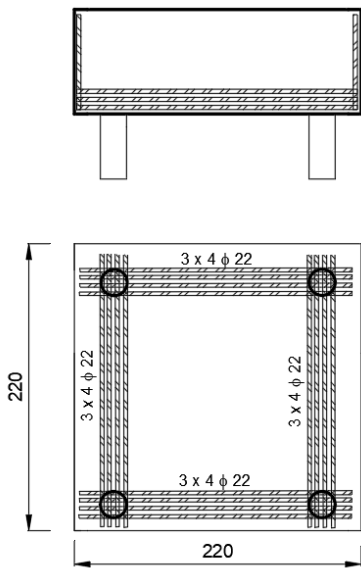
$$A_{sd,tie} = \frac{\gamma_f * T_1}{f_{yd}} = \frac{1.4 * 1,250}{50/1.15} = 40.25\ cm^2\ (3\ layers\ of\ 4\ No.\ 22)$$

adopting steel bar with diameter $d = 22\ mm$ with 12 bars ($A_{s,effective} = 45.60\ cm^2$)

In the inclined strut, the verification of the compressive stresses is performed according to

$$Concreto\ C32 - f_{ck} = 32\ MPa$$

$$E_{ci} = \alpha_E * \alpha_i * 5600 * \sqrt{f_{ck}} = 1.0 * 0.88 * 5600 * \sqrt{32} = 27,877\ MPa$$

and the area of the strut required for the design strength of the concrete not to be exceeded:

$$A_{cd,strut} = \frac{\gamma_f * C_1}{0.8 * f_{cd}} = \frac{1.4 * 2,031}{0.8 * (3.2/1.4)} = 1.555\ cm^2$$

By way of comparison, in [26], the results of this sizing are $A_{sd,tie} = 41.66\ cm^2$ and $A_{cd,strut} = 1,659\ cm^2$. The differences in values (3.5% and 6.3, respectively) are due to different calculation criteria between the technical standards used, but values of the same order of magnitude can be considered. Fig. 12 shows the reinforcement arrangement for the pile cap.

Fig. 12: Reinforcement arrangement for the pile cap

The compliance history and the performance of the methods during the optimization procedure are plotted in Fig. 14. It can be seen in Fig. 14b that the performance index perfectly captures the changes in compliance and increases from unity to a maximum value of 2.3, stabilizing quickly around 2.1, the value at the optimal iteration.

The history of the optimization procedure via SESO and VFLSM for the bridge pier are shown in Fig. 1 and Fig. 16. The optimal topologies were achieved at iterations 82 and 100 with final volumes equal to 20% of the initial volume and a computational cost of 4,315.8 sec for SESO while VFLSM showed a computational cost of 5,486.5 sec.
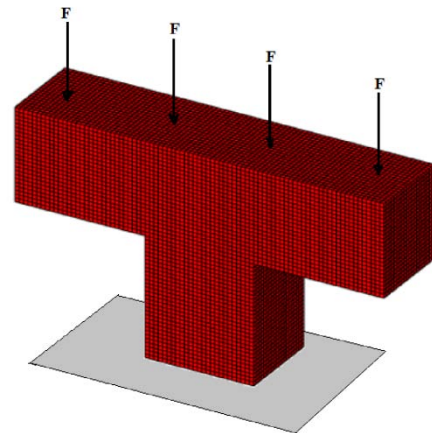

Fig. 13: Project domain of the Bridge pier

c) Example 3 – Bridge pier

The SESO and VFLSM methods using the MMA as accelerator are applied to a structure representing a column receiving loading from the bridge superstructure, represented by four vertical forces, as shown in Fig. 13. The concrete material properties, rejection ratio (RR), evolutionary ratio (ER) and filter radius are the same as in the previous example. For the numerical simulations, in the SESO method the bridge support is discretized using a fine mesh of 85x55x20 hexahedral elements of eight nodes, with reference side of 1 mm, while in the VFLSM method the mesh used has 85x20x55, totaling 93,500 tetrahedral finite elements.
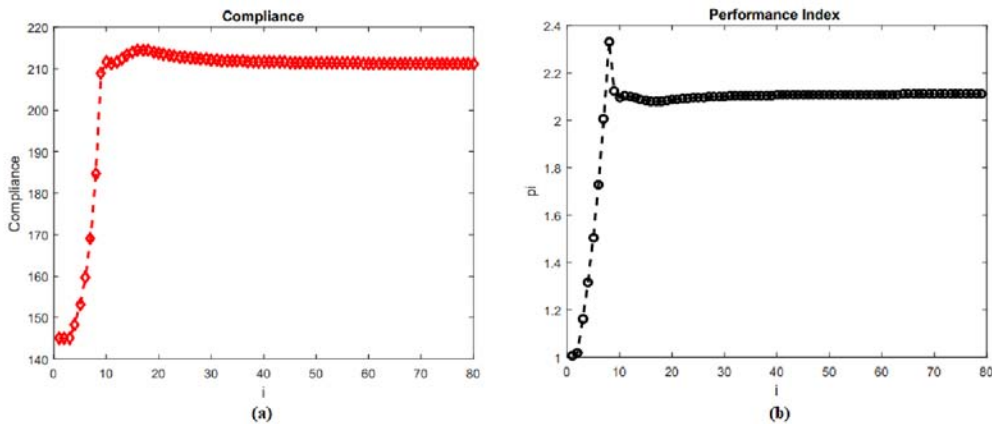

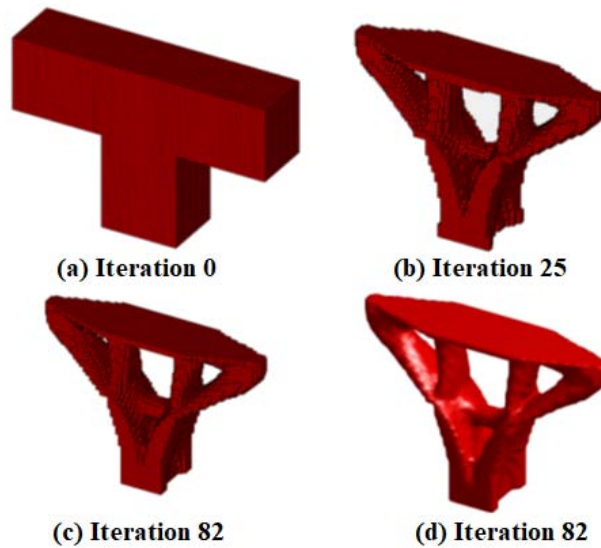
Fig. 14: Performance Index: topological history

Fig. 15: Optimization history of bridge pier with SESO: (a) initial structure; (b) topology at iteration 25; (c) optimal topology at iteration 82; (d) optimal topology (hexahedral elements)
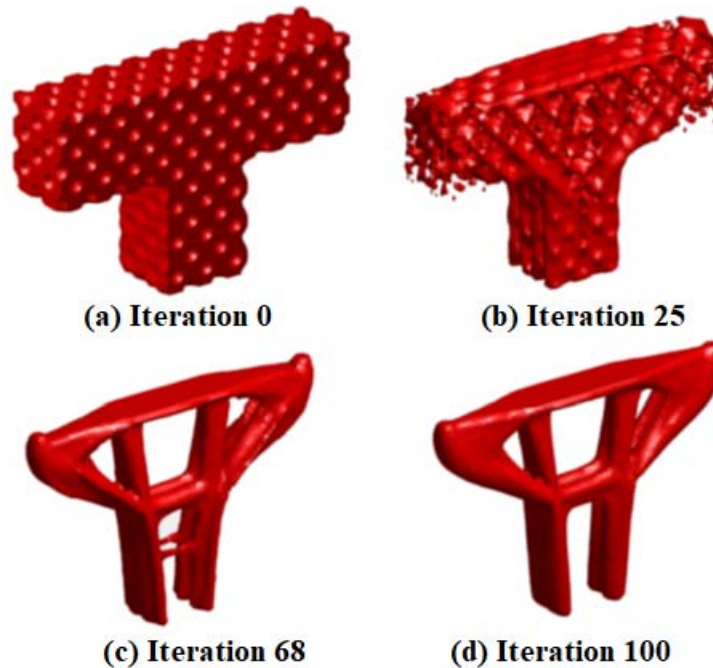

Fig. 16: Optimization history of bridge pier VFLSM: (a) initial structure; (b) topology at iteration 25; (c) optimal topology at iteration 68 (d) optimal topology (tetrahedral elements)

The optimal settings with highlights of the distinct regions by colors are presented in Fig. 17 for the two methods proposed in this paper. In these representations, a vertical axial force is expected to balance the symmetric external loads in the region of the base constraint. The applied vertical forces, in fact, are transferred to the column axis by means of two inclined struts and two vertical struts that merge into two in the proximity of the top region of the vertical element, driving the load distribution to the lower region where are the base supports. Note that the SESO method creates a unified region at the base while the VFLSM method sets up two parallel vertical paths. In addition, a horizontal tensile tie is arranged at the top of the body receiving the applied forces, which ensures the "T" geometry of the structure and configures the struts equilibrium in the load application zones. From a numerical point of view, the result obtained is optimal and configures the symmetry defined by the position of the design load. For automatic generation of STM models in the VFLSM method, it was necessary to implement the derivatives of von Mises stresses in the code proposed by [34]. Fig. 17b exhibits an optimal topology of VFLSM with tensile stress flows (blue) in the upper part and compression

stress flows (green) similar to those of the SESO method, Fig. 17a, highlighting the robustness of both methods for creating strut-and-tie models. With the objective of investigate the effects of D-regions, three holes were inserted in the horizontal element of the bridge pier structure, and the number of finite elements of the mesh was reduced to 88,700, as shown in Fig. 18. The optimal topologies of the SESO and VFLSM models are represented in Fig. 19, where the struts are represented by green color and the ties by blue color.

The optimum results obtained demonstrate that the presence of geometric discontinuities produces changes in the stress flows, that seek to contour the discontinuities, describing practically vertical struts in the horizontal body of the bridge pier from the points of load application. These struts bend below the openings to meet at the top of the vertical element, creating points of deviation that need to be equilibrated by tensile ties. In Fig. 19, it can be seen the representations of STM elements created as described.

This modification with the presence of the openings affects the STMs models significantly, and the real load transfer mechanism can change with the dimensions of the openings. The optimization histories are shown in Fig. 20 and Fig. 21, by the SESO and VFLSM formulations, respectively.
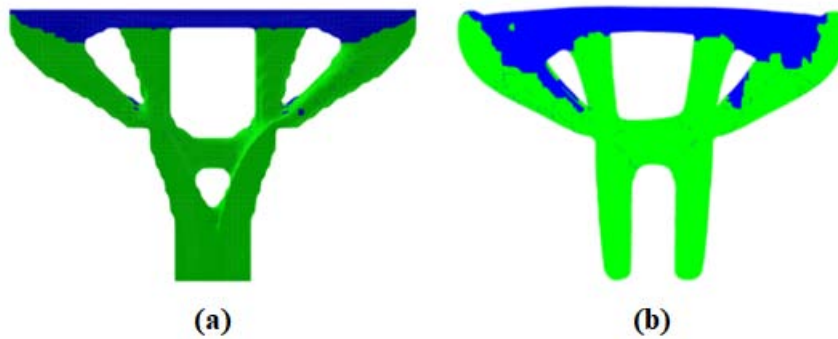

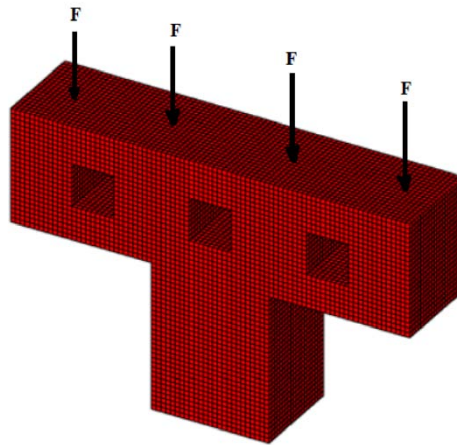*Fig. 17:* Bridge Pier: Strut-and-tie models (a) SESO and (b) VFLSM

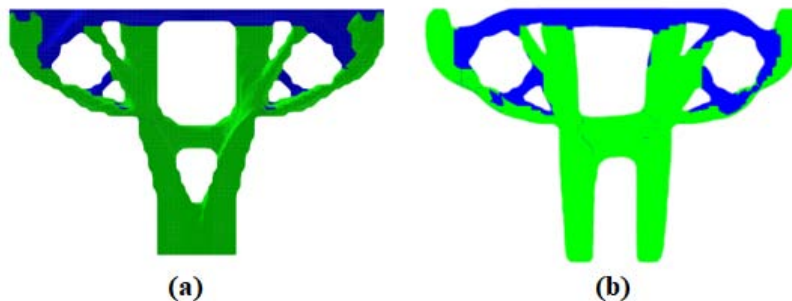*Fig. 18:* Bridge pier with three holes as structural discontinuities in horizontal braces

Fig. 19: Strut-and-tie model: (a) SESO and (b) VFLSM

(a) Iteration 0   (b) Iteration 25
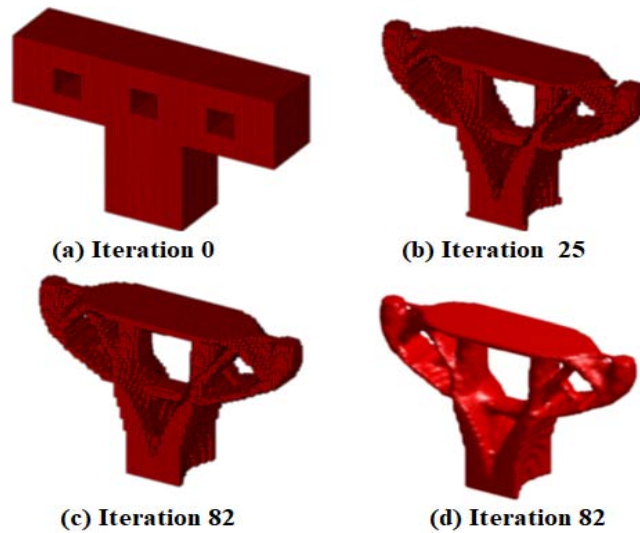
(c) Iteration 82   (d) Iteration 82

Fig. 20: Optimization history of bridge pier with openings SESO: (a) initial structure ; (b) topology at iteration 25; (c) optimal topology at iteration 70; (d) final optimal topology
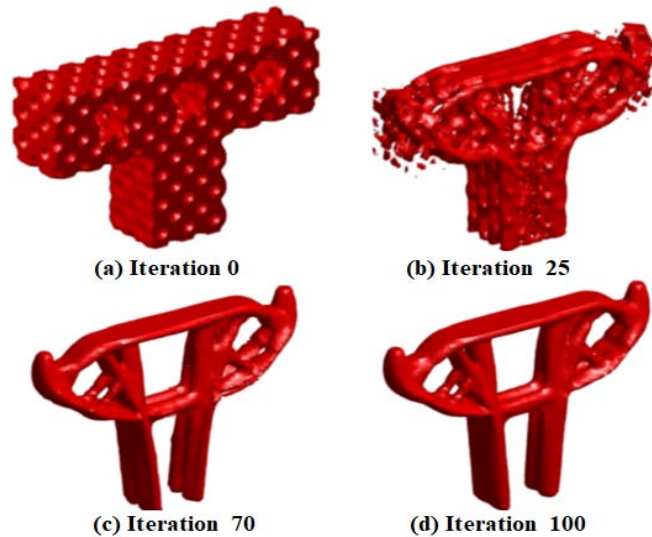

(a) Iteration 0   (b) Iteration 25

(c) Iteration 70   (d) Iteration 100

Fig. 21: Optimization history of bridge pier with openings VFLSM: (a) initial structure ; (b) topology at iteration 27; (c) optimal topology at iteration 70; (d) optimal topology

d) Example 4 – Single Corbel

    The SESO and VFLSM methods were also experimented with for modeling struts-and-ties in a single corbel attached to a column. A simple structure can eventually result in an intricate STM as the dimensions and load arrangements can be defined. The geometry and dimensions of the structure are shown in Fig. 22. This single corbel is subjected to a concentrated load of 1 kN. The compressive strength of the concrete used in this example is 32 MPa. Young's modulus of the concrete E = 28,567 MPa and the Poisson's ratio $v = 0.15$ were defined in the analysis. A prescribed fraction volume V = 0.22 m³ and an evolution ratio of ER = 2% was specified in the optimization process.

    In the SESO method the structure was discretized with a mesh of 44x12x108 unit hexahedral finite elements. The performance of the structure was monitored throughout the optimization procedure and, despite the breaks in the load transfer mechanisms due to element removal, the structure did not present failure modes and the performance index remained higher than 1, stabilizing at 1.6. In the VFLSM method, the same mesh was used, totaling 57,024 tetrahedral elements. Figures 23a, b, c and d show that the optimal topologies obtained by the two models are different and checkerboard patterns were not detected. It is noted in observation made in the deep beam example that both formulations, SESO and VFLSM, define settings differently for elements of strut-and-tie models. Discrete elements are configured on the side faces of the models

in different regions, while complete planes are shaped in other regions, with no common convention between the two formulations. The presented results show that both SESO-3D and VFLSM-3D are able to provide the prediction of the load transfer mechanism in reinforced concrete structures, even considering the structural domain thickness in the configuration of the component elements of the models.
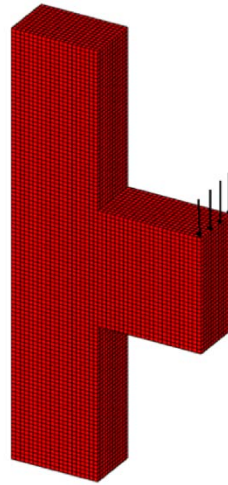
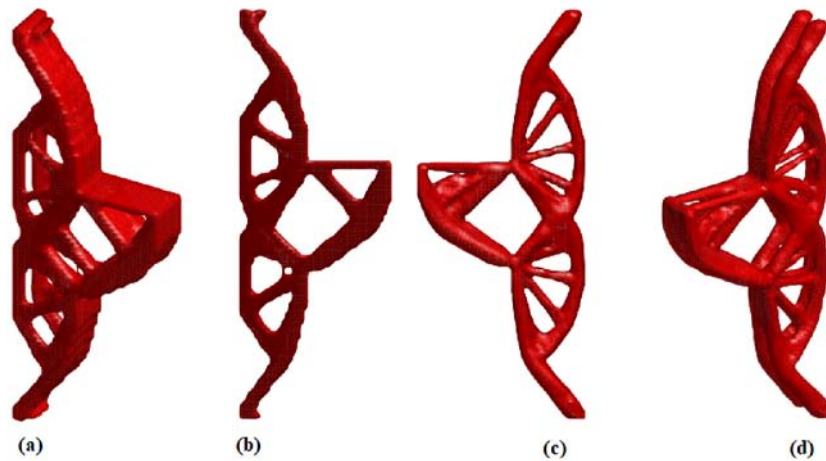*Fig. 22:* Single Corbel: Project Domain

Fig. 23: Single Corbel, optimal topology: (a) e (b) SESO (c) and (d) VFLSM

The STMs are presented in Fig. 24, it can be seen that these models are different and capable of clearly representing the location of the struts, ties and nodal zones. These results can be compared with those presented by [16] and [26]. It is also highlighted that the parameters of the MMA optimizer were changed to $\zeta \leq 0.98, \xi \leq 1.25$ e $\varsigma \leq 0.75$ proportion a more feasible topology for design. Fig. 24b shows the optimal setting of the VFLSM used for automatic creation of the STM models; both formulations exhibit distinct tensile (blue) and compressed (green) regions, even in the width of the structural domain. Table 1 highlights the computational cost of SESO and VFSLM in all the examples presented in this paper evidencing the better performance for SESO-OC and SESO-MMA compared to VFLSM-MMA.
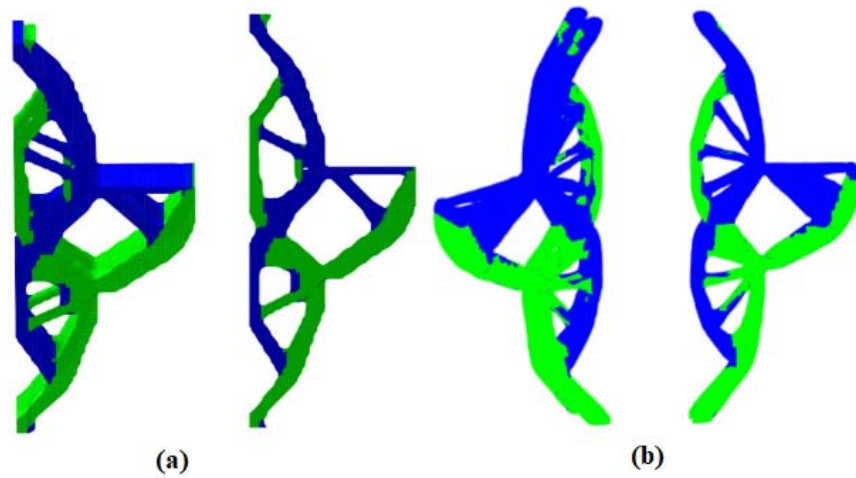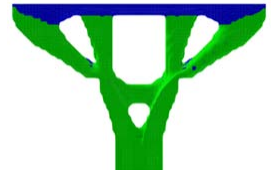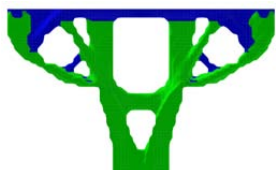
Fig. 24: Single Corbel, Strut-and-tie model: (a) SESO; (b) VFSLM

Table 1: Strut-and-tie Models and Computational Cost

Structure	Computational Cost (minute) (SESO-OC)	Computational Cost (minute) (SESO-MMA)	Computational Cost (minute) (VFLSM)	Strut-and-tie Models
Deep beam with opening	90.7	109.8	229.81	
Pile Cap	21.4	38.0	64.2	
Bridge pier	57.9	95.0	159.3	
Bridge pier with three holes	56.5	95.9	158.6	
Single Corbel	45.4	71.9	103.7	

V. Conclusions

This paper aimed to extend the application of TO in 3D elasticity to obtain the best solution to STM problems. It brought some processes as innovation, such as the use of the SESO method and the VFLSM employed in conjunction with the OC and MMA methods to accelerate and stabilize the analyses; so that, the first method demonstrated to be more efficient when employed with the SESO, about 2 to 3 times faster in all the examples evaluated. It is highlighted that in these processes the incorporation of the linear solution by the conjugate gradient method with the incomplete Cholesky preconditioner further enhanced the computational cost. In the automated generation of the final designs of the STM, the procedure of obtaining struts and ties computed by the partial derivatives of the stresses of each element was applied highlighting that this novelty is easy to implement and the use of a spatial modal filter in the stress field was enough to completely eliminate the checkerboard. From the automatic generations performed, it was possible to design an example according to the recurring norm in an expeditious manner, in which the required reinforcement areas were evaluated and compared, demonstrating a good similarity. All codes were implemented in the high level language Matlab, which is easily accessible and extensible for future incorporation of other more realistic models, such as a rheological model more suitable for concrete. The study of STM using optimization applied to both materials (steel and concrete), leading to dimensioning and detailing of RC structural elements under the reliability-based topology optimization (RBTO) paradigm, taking advantage of the efficiency and stability of the procedures, are the highlights in the formulations developed in this paper.

Acknowledgment

References Références Referencias

1. Schlaich, J., Schafer, K., Jennewein, M. Toward a consistent design of structural concrete. PCI-Journal, vol. 32, nr.3, p. 74 – 150, May/June, 1987.
2. Schlaich J, Schäfer K (1991) Design and detailing of structural concrete using strut-and-tie models. Struct Eng 69(6):113–125.
3. Schlaich M, Anagnostou, G (1990) Stress fields for nodes of strut-and-tie models. Struct Eng 116(1):13–23.
4. Marti P (1980) On plastic analysis of reinforced concrete. Institute of Structural Engineers, report no. 104.
5. Marti, P. (1985). "Truss models in detailing." Concr. Int., 7(12), 66-73.
6. Muttoni, A., Schwartz, J., Thürlimann, B. Design of Concrete Structures with Stress Fields, 1st ed., Birkhäuser Verlag, Basel, 1996.
7. Indu Geevar; Devdas Menon. Strength of Reinforced Concrete Pier Caps—Experimental Validation of Strut-and-Tie Method (2019). ACI Structural Journal, 116 (1), 261-274.
8. Tuchscherer, Robin G.; Birrcher, David B.; Williams, Christopher S.; Deschenes, Dean J.; Bayrak, Oguzhan. Evaluation of existing strut-And-tie methods and recommended improvements. ACI structural journal, 2014, Vol.111 (6), p.1451-1460.
9. Chen, B. S., Hagenberger, M. J., Breen, J. E.. Evaluation of Strut-and-Tie Modeling Applied to Dapped Beam with Opening. ACI Structural Journal, 2002, vol. 99, pp. 445–450.
10. Maxwell, B. S., Breen, J. E. Experimental Evaluation of Strut-and-Tie Model Applied to Deep Beam with Opening. ACI Structural Journal, 2000, vol. 97, pp. 142–148.
11. ASCE-ACI Committee 445, "Recent Approaches to Shear Design of Structural Concrete," Journal of Structural Engineering, V. 124, No. 12, Dec. 1998, pp. 1375-1417.
12. American Association of State Highway and Transportation Officials. AASHTO LRFD Bridge Design Specifications; American Association of State Highway and Transportation Officials: Washington, DC, USA, 2007.
13. Deutsche Norm, Concrete, Reinforced and Prestressed Concrete Structures-Part 1:3 Design and Construction, Corrigenda to DIN 1045-1:2001-07; German Institute for Standardisation (Deutsches Institut für Normung): Berlin, Germany, 2008.
14. Canadian Standards Association (CSA). Design of Concrete Structures for Buildings (CAN3-A23.3-M84); CSA: Toronto, ON, Canada, 1984.
15. Yi Xia; Matthijs Langelaar; Max A. N. Hendriks. Optimization-based three-dimensional strut-and-tie model generation for reinforced concrete. Computer-Aided Civil and Infrastructure Engineering, 36:526-543, 2021.
16. Bruggi, M. Generating strut-and-tie patterns for reinforced concrete structures using topology optimization. Computers and Structures, 87:1483-1495, 2009.
17. Bogomolny, M.; Amir, O. Conceptual design of reinforced concrete structures using topology

optimization with elastoplastic material modeling. Int. J. Numer. Meth. Engng 2012; 90:1578–1597.

18. Vaquero, Sebastian F., and Raul D. Bertero. "Automatic Generation of Proper Strut-and-Tie Model." ACI Structural Journal, vol. 117, no. 6, Nov. 2020, pp. 81.

19. Ali, M. A., and White, R. N. Automatic Generation of Truss Model for Optimal Design of Reinforced Concrete Structures. ACI Structural Journal, V. 98, No. 4, July-Aug. 2001, pp. 431-442.

20. Kwak, H. G., & Noh, S. H. (2006). Determination of strut-and-tie models using evolutionary structural optimization. *Engineering Structures*, *28*(10), 1440-1449.

21. Liang, Q. Q., Y. M. Xie, and G. P. Steven. 2000. "Topology Optimization of Strut-and-Tie Models in Reinforced Concrete Structures Using an Evolutionary Procedure." ACI Structural Journal 97 (2): 322–330.

22. Liang, Q. Q., Y. M. Xie, and G. P. Steven. 2001. "Generating Optimal Strut-and-Tie Models in Prestressed Concrete Beams by Performance-Based Optimization." ACI Structural Journal 98 (2): 226–232.

23. Liang, Q. Q., B. Uy, and G. P. Steven. 2002. "Performance-Based Optimization for Strut-Tie Modeling of Structural Concrete." Journal of Structural Engineering 128 (5): 815–823.

24. Chen BS, Hagenberger MJ, Breen JE. Evaluation of strut-and-tie model applied to deep beam with opening. ACI Structural Journal 2002;99(2): 445–50.

25. Zhong, J. T., Wang, L., Deng, P., & Zhou, M. (2017). A new evaluation procedure for the strut-and-tie models of the disturbed regions of reinforced concrete structures. *Engineering Structures*, *148*, 660-672.

26. Shobeiri, V., & Ahmadi-Nedushan, B. Bi-directional evolutionary structural optimization for strut-and-tie modelling of three-dimensional structural concrete. Engineering Optimization, 49(12), 2055-2078, 2017.

27. Leu, L. J., Huang, C. W., Chen, C. S., & Liao, Y. P. (2006). Strut-and-tie design methodology for three-dimensional reinforced concrete structures. *Journal of structural Engineering, New York*, *132*(6), 929.

28. Almeida, V. S., Simonetti, H. L., & Neto, L. O. (2013). Comparative analysis of strut-and-tie models using Smooth Evolutionary Structural Optimization. *Engineering Structures*, *56*, 1665-1675.

29. Sethian, J. A., & Wiegmann, A. (2000). Structural boundary design via level set and immersed interface methods. Journal of Computational Physics, 163, 489–528. http://dx.doi.org/10.1006/jcph.2000.6581.

30. Wang MY, Wang X, Guo D (2003) A level set method for structural topology optimization. Comput Methods Appl Mech Eng 192: 227–246.

31. Allaire G, Jouve F, Toader AM (2004) Structural optimization using sensitivity analysis and a level-set method. J Comput Phys 194(1):363–393.

32. Luo Z, Tong L, Kang Z (2009a) A level set method for structural shape and topology optimization using radial basis functions. Comput Struct 87:425–434.

33. van Dijk NP, Maute K, Langelaar M, van Keulen F (2013) Level-set methods for structural topology optimization: a review. Struct Multidiscip Optim 48:437–472.

34. Wang, Y., & Kang, Z. (2021). MATLAB implementations of velocity field level set method for topology optimization: an 80-line code for 2D and a 100-line code for 3D problems. Structural and Multidisciplinary Optimization, 64, 4325-4342.

35. Wang Y, Kang Z, Liu P (2019) Velocity field level-set method for topological shape optimization using freely distributed design variables. Int J Numer Methods Eng 120:1411–1427.

36. Huang X, Zuo ZH, Xie YM. Evolutionary topological optimization of vibrating continuum structures for natural frequencies. Computer Structure. 2010;88(5– 6):357–64.

37. Strömberg N. Topology optimization of structures with manufacturing and unilateral contact constraints by minimizing an adjustable compliance– volume product. Struct Multidiscip Optim 2010;42(3):341–50.

38. Yamasaki S, Nomura T, Kawamoto A, Sato K, Izui K, Nishiwaki S. A level set based topology optimization method using the discretized signed distance function as the design variables. Struct Multidisc Optim 2009;41(5):685–98.

39. Allaire G, Jouve F, Toader A-M. Structural optimization by the level-set method. In: Colli P, Verdi C, Visintin A. editors. Free boundary problems. Birkhäuser Basel; 2003. p. 1–5.

40. Dunning PD, Stanford BK, Kim HA. Coupled aerostructural topology optimization using a level set method for 3D aircraft wings. Struct Multidiscip Optim 2014;51(5):1113–32.

41. Coelho PG, Rodrigues HC. Hierarchical topology optimization addressing material design constraints and application to sandwich-type structures. Struct Multidiscip Optim 2015;52(1):91–104.

42. Xie YM, Steven GP. A simple evolutionary procedure for structural optimization, Computers & Structures, Vol. 49, n. 5, p. 885-896, 1993.

43. Simonetti HL, Almeida VS, Neto LO. A smooth evolutionary structural optimization procedure applied to plane stress problem. Eng Struct 2014; 75:248–58.

44. Svanberg, K. 1987: Method of moving asymptotes — a new method for structural optimization. *Int. J. Num. Meth. Eng.24,* 359–373.

45. Victoria, M., Querin, O. M. & Martí, P. Generation of strut-and-tie models by topology design using

different material properties in tension and compression. *Struct Multidisc Optim* 44, 247–258 (2011). https://doi.org/10.1007/s00158-011-0633-z.

46. Kong FK, Sharp GR. Structural idealization for deep beams with web openings. Magazine Concrete Res 1977; 29:81–91.

47. Simonetti, H. L.; Almeida, V. S.; de Assis das Neves, F.; Del Duca Almeida, V.; de Oliveira Neto, L. Reliability-Based Topology Optimization: An Extension of the SESO and SERA Methods for Three-Dimensional Structures. Appl. Sci. 2022, 12, 4220. https://doi.org/10.3390/app12094220.